

# Spectroscopic Characterization of Disulfiram and Nicotinic Acid after Biofield Treatment

Mahendra Kumar Trivedi<sup>1</sup>, Alice Branton<sup>1</sup>, Dahryn Trivedi<sup>1</sup>, Gopal Nayak<sup>1</sup>, Khemraj Bairwa<sup>2</sup> and Snehasis Jana<sup>2\*</sup>

<sup>1</sup>Trivedi Global Inc., 10624 S Eastern Avenue Suite A-969, Henderson, NV 89052, USA

<sup>2</sup>Trivedi Science Research Laboratory Pvt. Ltd., Hall-A, Chinar Mega Mall, Chinar Fortune City, Hoshangabad Rd., Bhopal- 462026, Madhya Pradesh, India

## Abstract

Disulfiram is being used clinically as an aid in chronic alcoholism, while nicotinic acid is one of a B-complex vitamin that has cholesterol lowering activity. The aim of present study was to investigate the impact of biofield treatment on spectral properties of disulfiram and nicotinic acid. The study was performed in two groups i.e., control and treatment of each drug. The treatment groups were received Mr. Trivedi's biofield treatment. Subsequently, spectral properties of control and treated groups of both drugs were studied using Fourier transform infrared (FT-IR) and Ultraviolet-Visible (UV-Vis) spectroscopic techniques. FT-IR spectrum of biofield treated disulfiram showed the shifting in wavenumber of C-H stretching from 1496 to 1506  $\text{cm}^{-1}$  and C-N stretching from 1062 to 1056  $\text{cm}^{-1}$ . The intensity of S-S dihedral bending peaks (665 and 553  $\text{cm}^{-1}$ ) was also increased in biofield treated disulfiram sample, as compared to control. FT-IR spectra of biofield treated nicotinic acid showed the shifting in wavenumber of C-H stretching from 3071 to 3081  $\text{cm}^{-1}$  and 2808 to 2818  $\text{cm}^{-1}$ . Likewise, C=C stretching peak was shifted to higher frequency region from 1696  $\text{cm}^{-1}$  to 1703  $\text{cm}^{-1}$  and C-O (COO<sup>-</sup>) stretching peak was shifted to lower frequency region from 1186 to 1180  $\text{cm}^{-1}$  in treated nicotinic acid.

UV spectrum of control and biofield treated disulfiram showed similar pattern of UV spectra. Whereas, the UV spectrum of biofield treated nicotinic acid exhibited the shifting of absorption maxima ( $\lambda_{\text{max}}$ ) with respect of control i.e., from 268.4 to 262.0 nm, 262.5 to 256.4, 257.5 to 245.6, and 212.0 to 222.4 nm.

Over all, the FT-IR and UV spectroscopy results suggest an impact of biofield treatment on the force constant, bond strength, and dipole moments of treated drugs such as disulfiram and nicotinic acid that could led to change in their chemical stability as compared to control.

**Keywords:** Disulfiram; Nicotinic acid; Biofield treatment; Fourier transform infrared spectroscopy; Ultraviolet spectroscopy

## Introduction

Disulfiram [bis(diethylthiocarbamoyl)disulphide] is an antabuse drug, being used clinically as an aid to the treatment of chronic alcoholism. It is the first drug approved by US Food and Drug Administration to treat the alcohol addiction [1]. Alcohol (ethanol) transforms into acetaldehyde by alcohol dehydrogenase enzyme, which further oxidized to acetic acid by acetaldehyde dehydrogenase (ADH) enzyme [2]. Disulfiram inhibits the ADH enzyme. As a result, the blood concentration of acetaldehyde increases and causes an unpleasant effect, thus increase the patient's motivation to remain abstinent [3]. In addition to this, disulfiram is reported for protozoacidal effect *in vitro* study [4,5]. Recently, disulfiram has shown the reactivity to latent HIV-1 expression in a primary cell model of virus latency and presently it is assessed in a clinical trial for its potential to diminish the latent HIV-1 reservoir in patients combination with antiretroviral therapy [6].

Nicotinic acid or niacin is one of the B-complex vitamins (Vitamin B<sub>3</sub>) that has cholesterol lowering activity. Recent studies showed that therapeutic doses of nicotinic acid induce a profound alteration in plasma concentration of several lipids and lipoproteins, resulting in a greater ability to increase high-density lipoprotein (HDL) cholesterol [7]. Nicotinic acid favorably affects apolipoprotein (apo), very-low-density lipoprotein (VLDL), low-density lipoprotein (LDL) and HDL [7,8].

The exact mechanism of nicotinic acid activity is unknown. However, new findings indicate that nicotinic acid inhibits directly and non-competitively to the triglycerides synthesis enzyme i.e., hepatocyte diacylglycerol acyltransferase-2, which causes acceleration of intracellular hepatic apo B degradation and thus decrease secretion

of VLDL and LDL [9]. Several evidence suggest that nicotinic acid administered either alone or in combination with other cholesterol-lowering medicines can reduce the risk of cardiovascular and atherosclerosis diseases. The clinical uses of nicotinic acid are somewhat limited due to some harmless but unpleasant side effects like cutaneous flushing phenomenon, nausea, vomiting and headache [10]. The chemical and physical stability of pharmaceutical drugs or products are most desired attributes of quality that potentially affect the efficacy, safety and shelf life of drugs [11]. Hence, it is essential to find out an alternate approach, which could enhance the stability of drugs by altering the structural and bonding properties of these compounds.

Contemporarily, biofield treatment is reported to alter the spectral properties of various pharmaceutical drugs like paracetamol, piroxicam, metronidazole, and tinidazole; likewise physical, and structural properties of various metals i.e., tin, lead etc. [12-14]. The conversion of mass into energy is well known in literature for hundreds of years that was further explained by Hasenohrl and Einstein [15,16]. According to Maxwell [17], every dynamic process in the human body had an electrical significance, which generates magnetic field in the human body [17].

**\*Corresponding author:** Snehasis Jana, Trivedi Science Research Laboratory Pvt. Ltd., Hall-A, Chinar Mega Mall, Chinar Fortune City, Hoshangabad Rd, Bhopal-462026, Madhya Pradesh, India, Tel: +91-755-6660006; E-mail: [publication@trivedisrl.com](mailto:publication@trivedisrl.com)

**Received** July 21, 2015; **Accepted** August 07, 2015; **Published** August 14, 2015

**Citation:** Trivedi MK, Branton A, Trivedi D, Nayak G, Bairwa K, et al. (2015) Spectroscopic Characterization of Disulfiram and Nicotinic Acid after Biofield Treatment. J Anal Bioanal Tech 6: 265 doi:10.4172/2155-9872.1000265

**Copyright:** © 2015 Trivedi MK, et al. This is an open-access article distributed under the terms of the Creative Commons Attribution License, which permits unrestricted use, distribution, and reproduction in any medium, provided the original author and source are credited.

This electromagnetic field of the human body is known as biofield and energy associated with this field is known as biofield energy [18,19]. Mr. Trivedi has the ability to harness the energy from environment or universe and can transmit into any living or nonliving object around this Globe. The object(s) always receive the energy and responding into useful way, this process is known as biofield treatment.

Mr. Mahendra Kumar Trivedi's biofield treatment (The Trivedi Effect®) has considerably changed the physicochemical, thermal and structural properties of metals and ceramics [14,20,21]. Growth and anatomical characteristics of some plants were also increased after biofield treatment [22,23]. Further, biofield treatment has showed the significant effect in the field of agriculture science [24,25] and microbiology [26,27].

Considering the impact of biofield treatment on physical and structural property of metals and ceramics, the present study was aimed to evaluate the impact of biofield treatment on spectral properties of disulfiram and nicotinic acid. The effects were analyzed using Fourier transform infrared (FT-IR) and Ultraviolet-Visible (UV-Vis) spectroscopic techniques.

## Materials and Methods

### Study design

The disulfiram and nicotinic acid (Figure 1) samples were procured from Sigma-Aldrich, MA, USA; and each drug was divided into two parts i.e., control and treatment. The control samples were remained as untreated, and treatment samples were handed over in sealed pack to Mr. Trivedi for biofield treatment under laboratory condition. Mr. Trivedi provided this treatment through his energy transmission process to the treated groups without touching the sample [12,13]. The control and treated samples of disulfiram and nicotinic acid were evaluated using FT-IR and UV-Vis spectroscopy.

### FT-IR spectroscopic characterization

FT-IR spectra were recorded on Shimadzu's Fourier transform infrared spectrometer (Japan) with frequency range of 4000-500  $\text{cm}^{-1}$ . The FT-IR spectroscopic analysis of both control and treated samples of disulfiram and nicotinic acid were carried out to evaluate the impact of biofield treatment at atomic level like force constant and bond strength [28].

### UV-Vis spectroscopic analysis

UV spectra of disulfiram and nicotinic acid were recorded on Shimadzu UV-2400 PC series spectrophotometer with 1 cm quartz cell and a slit width of 2.0 nm. The analysis was carried out using wavelength in the range of 200-400 nm. The analysis was performed to determine the effect of biofield treatment on structural properties of treated drugs [28].

## Results and Discussion

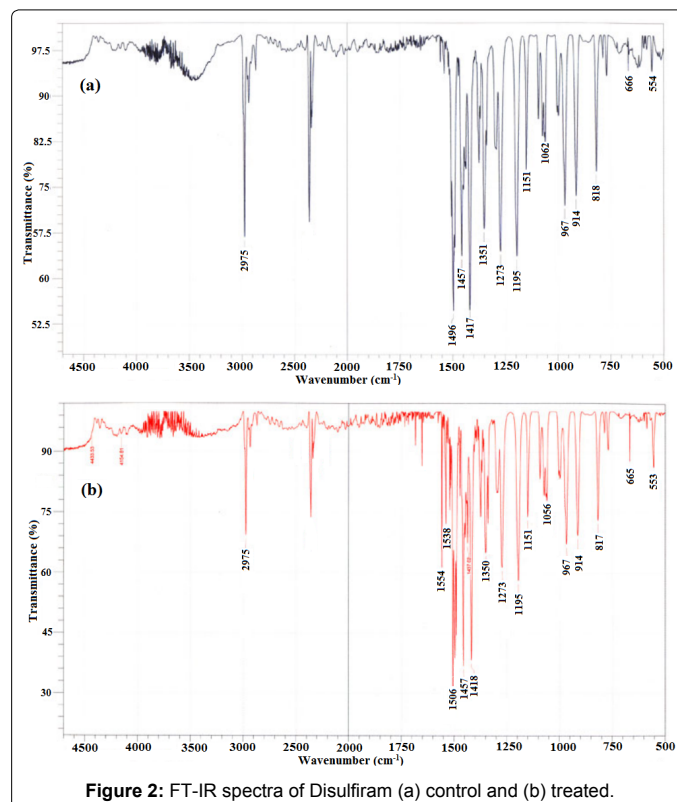
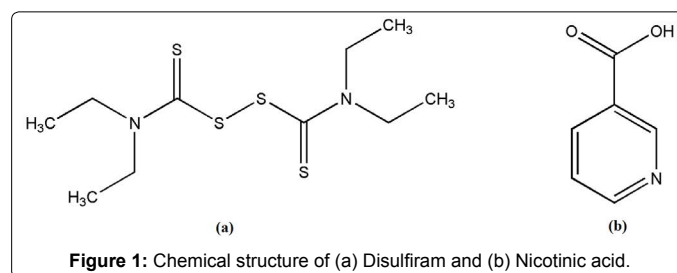
### FT-IR spectroscopic analysis

Vibrational spectral assignment was performed on the recorded FT-IR spectra (Figure 2) based on theoretically predicted wavenumber and presented in Table 1. The FT-IR spectrum of control disulfiram sample (Figure 2a) showed the characteristic vibrational peak at 2975  $\text{cm}^{-1}$  that was assigned to C-H ( $\text{CH}_3$ ) stretching. Another characteristic peak observed at 1496  $\text{cm}^{-1}$  was attributed to C-H symmetrical deformation vibrations. The absorption peaks appeared at 1351-1457  $\text{cm}^{-1}$  was assigned to  $\text{CH}_2$ - $\text{CH}_3$  deformations. The vibrational peaks

at 1273  $\text{cm}^{-1}$  and 1151-1195  $\text{cm}^{-1}$  were assigned to C=S stretching and C-C skeletal vibration, respectively. Further, IR peaks observed at 967-1062  $\text{cm}^{-1}$  and 818-914  $\text{cm}^{-1}$  were attributed to C-N stretching and C-S stretching, respectively. The vibrational peaks appeared at 554-666  $\text{cm}^{-1}$  was assigned to S-S dihedral bending. The FT-IR data of control disulfiram was well supported by the literature data [29].

The FT-IR spectrum of biofield treated disulfiram (Figure 2b) showed the vibrational peak at 2975  $\text{cm}^{-1}$ , which was assigned to  $\text{CH}_3$  stretching. Vibrational peak appeared at 1506  $\text{cm}^{-1}$  was assigned to C-H symmetrical deformation vibrations. Likely, the IR peaks at 1350-1457  $\text{cm}^{-1}$  were attributed to  $\text{CH}_2$ - $\text{CH}_3$  deformations. The vibrational peaks appeared at 1273  $\text{cm}^{-1}$  and 1151-1195  $\text{cm}^{-1}$  were assigned to C=S stretching and C-C skeletal vibration, respectively. The IR peaks observed at 967-1056  $\text{cm}^{-1}$  and 817-914  $\text{cm}^{-1}$  were attributed to C-N stretching and C-S stretching, respectively. The vibrational peaks at 553-665  $\text{cm}^{-1}$  were assigned to S-S dihedral bending.

Altogether, the FT-IR data of biofield treated disulfiram (Figure 2b) showed the shifting in frequency of some bonds with respect to control spectra like C-H symmetrical deformation vibrations frequency was shifted from 1496 (control) to 1506 (treated)  $\text{cm}^{-1}$ . The frequency ( $\nu$ ) of vibrational peak depends on two factors i.e., force constant ( $k$ ) and



Wave number (cm <sup>-1</sup> )		Frequency Assignment
Control	Treated	
2975	2975	CH <sub>3</sub> stretching
1496	1506	C-H symmetrical deformation vibrations
1351-1457	1350-1457	CH <sub>2</sub> and CH <sub>3</sub> deformation
1273	1273	C=S stretching
1151-1195	1151-1195	C-C skeletal vibrations
967-1062	967-1056	C-N stretching
818-914	817-914	C-S stretching
554-666	553-665	S-S stretching

Table 1: FT-IR vibrational peaks observed in Disulfiram.

reduced mass ( $\mu$ ), which can be explained by following equation [30]

$$\nu = 1/2\pi c \sqrt{(k/\mu)}$$

here, c is speed of light.

If reduced mass is constant, then the frequency is directly proportional to the force constant; therefore, increase in frequency of any bond suggested a possible enhancement in force constant of respective bond and *vice versa* [28]. Based on this it is hypothesized that due to increase in frequency of C-H symmetrical deformation (1496 to 1506 cm<sup>-1</sup>), the C-H bond strength in treated disulfiram might also be increased with respect of control. Contrarily, the C-N stretching vibration in treated disulfiram was sifted to lower frequency region as compared to control i.e., from 1062 to 1056 cm<sup>-1</sup>. This could be referred to decrease in C-N bond strength after biofield treatment in compression to control. In addition, the intensity of IR peak appeared at 553-665 cm<sup>-1</sup> (S-S dihedral bending) in biofield treated sample was found to be increased, with respect of control peaks in the same frequency region. The intensity of vibrational peaks of particular bond depends on the ratio of change in dipole moment ( $\partial\mu$ ) to change in bond distance ( $\partial r$ ) i.e., the intensity is proportionally change with changes in dipole moment and inversely change with alteration in bond distance [31]. Based on this, it is speculated that ratio of  $\partial\mu/\partial r$  might be altered in S-S bonds (appeared in the frequency region of 553-665 cm<sup>-1</sup>) with the influence of biofield treatment as compared to control.

The vibrational spectral assignment of nicotinic acid was performed on the recorded FT-IR spectra (Figure 3) based on theoretically predicted wavenumber and presented in Table 2. The vibrational peaks appeared at 3071-2808 cm<sup>-1</sup> was assigned to C-H stretchings. The IR peaks observed at 1696-1710 cm<sup>-1</sup> and 1596 cm<sup>-1</sup> were assigned to C=O (COO<sup>-</sup>) asymmetrical stretching and C=C stretching, respectively. Absorption peaks appeared at 1417, 1323, and 1301 cm<sup>-1</sup> were attributed to C=N symmetric stretching, C=O symmetrical stretching, and C-N stretching, respectively. The C-O (COO<sup>-</sup>) stretching peak was assigned to IR bend observed at 1186 cm<sup>-1</sup>. Further, C-H in plane and out plane bending vibrations was assigned to peaks observed in the range of 1033-1114 cm<sup>-1</sup> and 642-812 cm<sup>-1</sup>, respectively. The FT-IR data of control nicotinic acid was well supported by the literature data [32,33].

The FT-IR spectrum of biofield treated nicotinic acid (Figure 3) showed the absorption bands at 2818-3081 cm<sup>-1</sup> that were assigned to C-H stretching. Vibrational peaks appeared at 1703-1714 cm<sup>-1</sup> and 1594 cm<sup>-1</sup> were assigned to C=O (COO<sup>-</sup>) asymmetric stretching and C=C stretching, respectively. Likewise, the IR peaks observed at 1417, 1324, and 1301 cm<sup>-1</sup> were assigned to C=N stretching, C=O (COO<sup>-</sup>) symmetric stretching, and C-N stretching, respectively. The IR absorption peak appeared at 1180 cm<sup>-1</sup> was attributed to C-O (COO<sup>-</sup>) stretching. Further, the C-H in plane and out plane bending vibrations

was assigned to IR peaks observed at 1037-1116 cm<sup>-1</sup> and 642-812 cm<sup>-1</sup>, respectively.

Overall, the FT-IR data of biofield treated nicotinic acid (Figure 3) showed the shifting in wavenumber of some bonds with respect to control sample. For instance, the C-H stretching towards higher frequency region i.e., from 3071 to 3081 cm<sup>-1</sup> and 2808 to 2818 cm<sup>-1</sup>. This could be due to increase in force constant of C-H bond. Likewise, a slight upstream shifting in C=O stretching peak from 1710 to 1714 cm<sup>-1</sup> and 1696 to 1703 cm<sup>-1</sup> in treated nicotinic acid also suggests an increase in force constant of C=O bond in treated sample as compared to control. Contrarily, a slight downstream shifting in wavenumber of treated nicotinic acid from 1186 to 1180 cm<sup>-1</sup> C-O (COO<sup>-</sup> stretching); and from 1033 to 1037 cm<sup>-1</sup> (=C-H in plane bending) suggests the decrease in force constant of C-O bond and decrease in rigidity of =C-H bond in treated sample as compared to control.

### UV-Vis spectroscopy

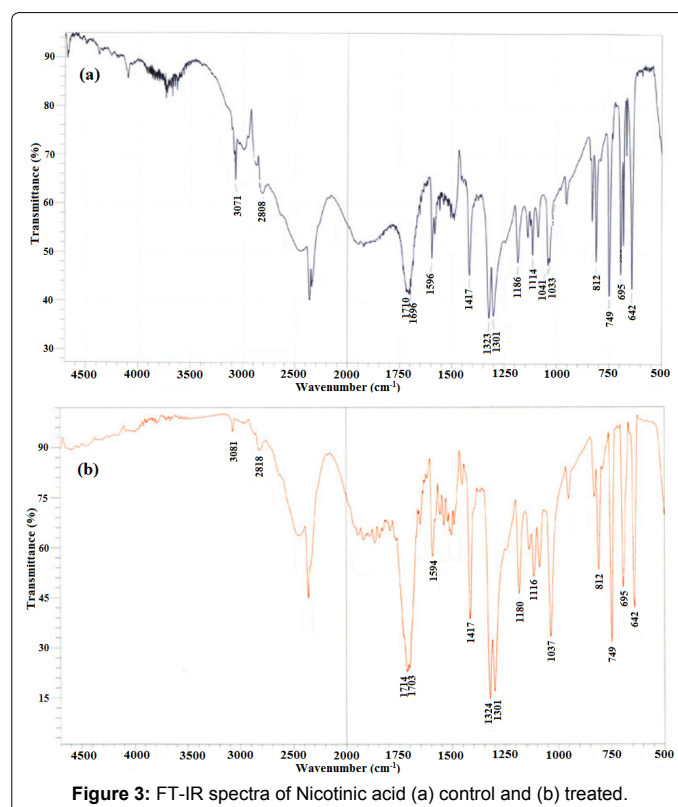


Figure 3: FT-IR spectra of Nicotinic acid (a) control and (b) treated.

Wave number (cm <sup>-1</sup> )		Frequency assignment
Control	Treated	
2808-3071	2818-3081	C-H stretching
1696-1710	1703-1714	C=O (COO <sup>-</sup> ) asymmetric stretching
1596	1594	C=C stretching
1417	1417	C=N stretching
1323	1324	C=O (COO <sup>-</sup> ) symmetric stretching
1301	1301	C-N stretching
1186	1180	C-OH (Ph-OH) stretching
1033-1114	1037-1116	=C-H in-plane bending
642-812	642-812	=C-H out of plane bending

Table 2: FT-IR vibrational peaks observed in Nicotinic acid.

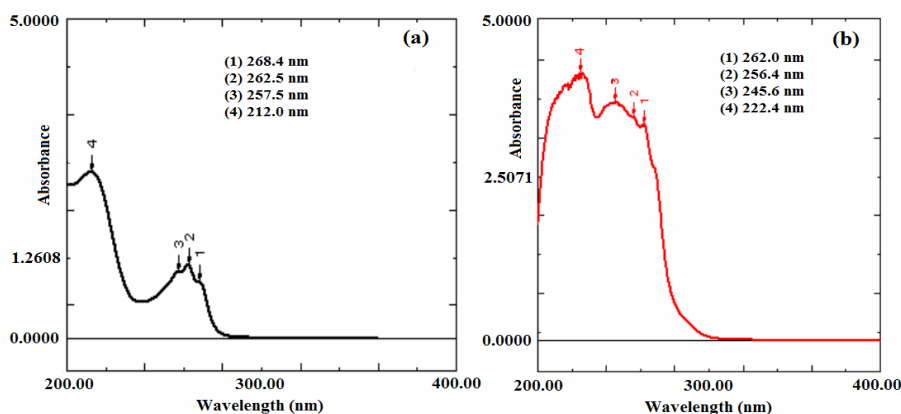


Figure 4: UV spectra of Nicotinic acid (a) control and (b) treated.

UV spectra of control and treated disulfiram showed a similar pattern of UV spectra with absorption maxima ( $\lambda_{\max}$ ) of 219.8, 250.2, and 281.6 nm in control and 220.8, 249.4, and 281.2 nm in treated sample. This indicates no significant change in the UV spectral property of treated disulfiram with respect to control sample. The UV spectra of control and treated nicotinic acid are showed in Figure 4. The UV spectrum of treated nicotinic acid (Figure 4) exhibited the shifting of absorption maxima ( $\lambda_{\max}$ ) from 268.4 to 262.0 nm, 262.5 to 256.4 nm, 257.5 to 245.6 nm, and 212.0 to 222.4 nm. The existing literature on principle of UV spectroscopy suggests that a compound can absorbs UV light due to presence of either or both conjugated pi ( $\pi$ ) -bonding systems ( $\pi$ - $\pi^*$  transition) and nonbonding electron system ( $n$ - $\pi^*$  transition) in the compound. The UV absorption phenomenon occurred when electrons travelled from low energy orbital (i.e.,  $\sigma$ ,  $n$ , and  $\pi$ ) to high energy orbital (i.e.,  $\sigma^*$  and  $\pi^*$ ). There is certain energy gap between  $\sigma$ - $\sigma^*$ ,  $\sigma$ - $\pi^*$ ,  $\pi$ - $\pi^*$  and  $n$ - $\pi^*$  orbitals. When this energy gap altered, the wavelength ( $\lambda_{\max}$ ) was also altered respectively [28]. Based on this, it is speculated that, due to influence of biofield treatment, the energy gap between  $\pi$ - $\pi^*$  and  $n$ - $\pi^*$  transition in nicotinic acid might be altered, which causes shifting of wavelength ( $\lambda_{\max}$ ) in treated nicotinic acid as compared to control. To the best of our knowledge, this is the first report showing an impact of biofield treatment on structural properties like force constant, bond strength, dipole moment of disulfiram and nicotinic acid.

## Conclusion

The FT-IR data of biofield treated disulfiram showed an alteration in the wavenumber of C-H and C-N stretching; whereas, wavenumbers of C-H, C=O, and C-O stretching, and =C-H bending were altered in biofield treated nicotinic acid, with respect of control. Also, the peak intensity at 553-665  $\text{cm}^{-1}$  (S-S dihedral bending) was increased in biofield treated disulfiram, as compared to control. This alteration in wavenumber referred to alteration in the force constant and bond strength of respective group. The UV spectral data of biofield treated nicotinic acid also support the possible change in the structural property with respect of control.

In conclusion, the results suggest a significant impact of biofield treatment on structural property like force constant, bond strength, dipole moment, and energy gap between bonding and nonbonding orbital of treated drug with respect to control.

## Acknowledgement

The authors would like to acknowledge the whole team of MGV Pharmacy College, Nashik for providing the instrumental facility. Authors would also like to thank Trivedi Science™, Trivedi Master Wellness™ and Trivedi Testimonials for their consistent support during the work.

## References

1. Zindel LR, Kranzler HR (2014) Pharmacotherapy of alcohol use disorders: Seventy-five years of progress. J Stud Alcohol Drugs Suppl 17: 79-88.
2. Svensson S, Some M, Lundsjo A, Helander A, Cronholm T, et al. (1999) Activities of human alcohol dehydrogenases in the metabolic pathways of ethanol and serotonin. Eur J Biochem 262: 324-329.
3. Cederbaum AI (2012) Alcohol metabolism. Clin Liver Dis 16: 667-685.
4. Nash T, Rice WG (1998) Efficacies of zinc-finger-active drugs against *Giardia lamblia*. Antimicrob Agents Chemother 42: 1488-1492.
5. Bouma MJ, Snowdon D, Fairlamb AH, Ackers JP (1998) Activity of disulfiram (bis(diethylthiocarbamoyl)disulphide) and ditiocarb (diethyldithiocarbamate) against metronidazole-sensitive and -resistant *Trichomonas vaginalis* and *Tritrichomonas foetus*. J Antimicrob Chemother 42: 817-820.
6. Doyon G, Zerbato J, Mellors JW, Sluis-Cremer N (2013) Disulfiram reactivates latent HIV-1 expression through depletion of the phosphatase and tensin homolog. AIDS 27: F7-F11.
7. Patel S (2013) A review of available cholesterol lowering medicines in South Africa. S Afr Pharm J 80: 20-25.
8. Gille A, Bodor ET, Ahmed K, Offermanns S (2008) Nicotinic acid: pharmacological effects and mechanisms of action. Annu Rev Pharmacol Toxicol 48: 79-106.
9. Kamanna VS, Kashyap ML (2008) Mechanism of action of niacin. Am J Cardiol 101: 20B-26B.
10. Bodor ET, Offermanns S (2008) Nicotinic acid: An old drug with a promising future. Br J Pharmacol 153: S68-S75.
11. Blessy M, Patel RD, Prajapati PN, Agrawal YK (2014) Development of forced degradation and stability indicating studies of drugs-A review. J Pharm Anal 4: 159-165.
12. Trivedi MK, Patil S, Shettigar H, Bairwa K, Jana S (2015) Effect of biofield treatment on spectral properties of paracetamol and piroxicam. Chem Sci J 6: 98.
13. Trivedi MK, Patil S, Shettigar H, Bairwa K, Jana S (2015) Spectroscopic characterization of biofield treated metronidazole and tinidazole. Med chem 5: 340-344.
14. Dabhade VV, Tallapragada RR, Trivedi MK (2009) Effect of external energy on atomic, crystalline and powder characteristics of antimony and bismuth powders. Bull Mater Sci 32: 471-479.

15. Hasenohrl F (1904) On the theory of radiation in moving bodies. *Ann Phys* 320: 344-370.
16. Einstein A (1905) Does the inertia of a body depend upon its energy-content? *Ann Phys* 18: 639-641.
17. Maxwell JC (1865) A dynamical theory of the electromagnetic field. *Phil Trans R Soc Lond* 155: 459-512.
18. Rubik B (2002) The biofield hypothesis: its biophysical basis and role in medicine. *J Altern Complement Med* 8: 703-717.
19. Rivera-Ruiz M, Cajavilca C, Varon J (2008) Einthoven's string galvanometer: the first electrocardiograph. *Tex Heart Inst J* 35: 174-178.
20. Trivedi MK, Patil S, Tallapragada RM (2013) Effect of biofield treatment on the physical and thermal characteristics of vanadium pentoxide powders. *J Material Sci Eng S11*: 001.
21. Trivedi MK, Patil S, Tallapragada RM (2014) Atomic, crystalline and powder characteristics of treated zirconia and silica powders. *J Material Sci Eng* 3: 144.
22. Patil SA, Nayak GB, Barve SS, Tembe RP, Khan RR (2012) Impact of biofield treatment on growth and anatomical characteristics of *Pogostemon cablin* (Benth.). *Biotechnology* 11: 154-162.
23. Nayak G, Altekar N (2015) Effect of biofield treatment on plant growth and adaptation. *J Environ Health Sci* 1: 1-9.
24. Lenssen AW (2013) Biofield and fungicide seed treatment influences on soybean productivity, seed quality and weed community. *Agricultural Journal* 8: 138-143.
25. Shinde V, Sances F, Patil S, Spence A (2012) Impact of biofield treatment on growth and yield of lettuce and tomato. *Aust J Basic & Appl Sci* 6: 100-105.
26. Trivedi MK, Patil S, Shettigar H, Bairwa K, Jana S (2015) Phenotypic and biotypic characterization of *Klebsiella oxytoca*: An impact of biofield treatment. *J Microb Biochem Technol* 7: 203-206.
27. Trivedi MK, Patil S, Shettigar H, Gangwar M, Jana S (2015) Antimicrobial sensitivity pattern of *Pseudomonas fluorescens* after biofield treatment. *J Infect Dis Ther* 3: 222.
28. Pavia DL, Lampman GM, Kriz GS (2001) Introduction to spectroscopy. 3rd edn, Thomson learning, Singapore.
29. Marciniak B, Dettlaff K, Naskrent M, Pietralik Z, Kozak M (2012) DSC and spectroscopic studies of disulfiram radiostability in the solid state. *J Therm Anal Calorim* 108: 33-40.
30. Stuart BH (2004) Infrared Spectroscopy: Fundamentals and applications (analytical techniques in the sciences (AnTs)). John Wiley & Sons Ltd, Chichester, UK.
31. Smith BC (1998) Infrared Spectral Interpretation: A systematic approach. CRC Press.
32. Jegannathan S, Mary MB, Ramakrishnan V, Thangadurai S (2014) Vibrational spectral studies of bis (nicotinic acid) hydrogen perchlorate. *Asian J Research Chem* 7: 67-71.
33. Karabacak M, Kurt M (2008) Comparison of experimental and density functional study on the molecular structure, infrared and Raman spectra and vibrational assignments of 6-chloronicotinic acid. *Spectrochim Acta A Mol Biomol Spectrosc* 71: 876-883.